

# The 0.1-100 keV spectrum and variability of Mkn421 in high state

A. Malizia<sup>1,2,3</sup>, M. Capalbi<sup>1,3</sup>, F. Fiore<sup>1,4</sup>, P. Giommi<sup>1,5</sup>, G. Gandolfi<sup>3,6</sup>,  
 A. Tesseri<sup>3,6</sup>, L. A. Antonelli<sup>1,4</sup>, R. C. Butler<sup>5</sup>, G. Celidonio<sup>3,6</sup>, A. Coletta<sup>3,6</sup>,  
 L. Di Ciolo<sup>3,6</sup>, J. M. Muller<sup>6,7</sup>, L. Piro<sup>8</sup>, S. Rebecchi<sup>3,6</sup>, D. Ricci<sup>3,6</sup>, R. Ricci<sup>3,6</sup>,  
 M. Smith<sup>6,7</sup>, V. Torroni<sup>3,6</sup>

<sup>1</sup> *BeppoSAX Science Data Center, Via Corcolle 19, I-00131 Roma, Italy*

<sup>2</sup> *Southampton University, SO17 1BJ, England*

<sup>3</sup> *Telespazio, Via Corcolle 19, I-00131 Roma, Italy*

<sup>4</sup> *Osservatorio Astronomico di Roma, Via dell'Osservatorio, I-00044 Monteporzio Catone, Italy*

<sup>5</sup> *ASI, Area Ricerca Scientifica, Roma, Italy*

<sup>6</sup> *BeppoSAX SOC, Via Corcolle 19, I-00131 Roma, Italy*

<sup>7</sup> *SRON, Sorbonnelaan 2, 3584 CA Utrecht, The Netherlands*

<sup>8</sup> *Istituto di Astrofisica Spaziale, CNR, Via Fosso Del Cavaliere, I-00133, Roma, Italy*

3 December 2017

## ABSTRACT

The results of a *BeppoSAX* TOO observation of the BL Lac object Mkn421 during a high intensity state are reported and compared with monitoring X-ray data collected with the *BeppoSAX* Wide Field Cameras (WFC) and the RXTE All Sky Monitor (ASM). The 0.1-100 keV spectrum of Mkn421 shows continuous convex curvature that can be interpreted as the high-energy end of the synchrotron emission. The source shows significant short-term temporal and spectral variability, which can be interpreted in terms of synchrotron cooling. The comparison of our results with those of previous observations when the source was a factor 3-5 fainter shows evidence for strong spectral variability, with the maximum of the synchrotron power shifting to higher energy during high states. This behaviour suggest an increase in the number of energetic electrons during high states.

**Key words:** galaxies; active; BL Lacertae objects

## 1 INTRODUCTION

Mkn421 is a bright, nearby ( $z=0.03$ ) BL Lac object classified as HBL (High energy peaked BL Lac, Padovani & Giommi 1996) since its Spectral Energy Distribution (SED) peaks (in a  $\nu f(\nu)$  vs  $\nu$  representation) in the UV/X-rays. Mkn421 is one of a few extragalactic objects (with Mkn501, 1ES2344+514 and PKS2155-304, all HBLs) so far detected at TeV energies e.g. Punch et al. 1992 where it shows tremendous variability, down to timescales of about 15 minutes (Gaidos et al. 1996). Mkn421 was repeatedly monitored with the Whipple, HEGRA and CAT Cherenkov telescopes and, whenever possible, simultaneously observed with X-ray satellites. The X-ray emission is also highly variable, with distinct differences between the soft and hard X-rays. Multi-wavelength campaigns have shown correlated flux changes

between the X-ray and the TeV region (Takahashi et al. 1996).

In this paper we report the results of a *BeppoSAX* (Boella et al. 1997a) TOO observation of Mkn421 during a high intensity state. The source was hard and showed significant temporal and spectral variability on timescales down to 500-1000 seconds. A comparison with previous *BeppoSAX* observations carried out when Mkn421 was less luminous also shows remarkable spectral variations. As seen in two other HBL BL Lacs, namely Mkn501 (Pian et al. 1998) and 1ES2344+514 (Giommi et al. 1999), both observed by *BeppoSAX* during high states, also in Mkn 421 the peak of the synchrotron power significantly moves to higher energy, well into the X-ray band. These findings exploit the unique *BeppoSAX* spectral coverage (from 0.1 up

to 300 keV) to observe emission from the high energy tail of the emitting electron distributions.

## 2 OBSERVATION AND DATA ANALYSIS

The *BeppoSAX* Narrow Field Instruments (NFI) observed Mkn421 on 22 June 1998 as part of a Target Of Opportunity (TOO) program dedicated to the study of different types of AGN in high states. Mkn421 was also observed earlier by *BeppoSAX* on April and May 1997 as part of the normal observation program. The TOO observation was triggered when Mkn421 was detected in one of the *BeppoSAX* Wide Field Cameras (WFC, Jager et al. 1997) at a flux level of  $\sim 20$  mCrabs, that is in a high state compared with previous observations. The WFC trigger is very effective (as demonstrated by the *BeppoSAX* Gamma Ray Burst experience, e.g. Costa 1998) since it allows a much faster response compared to other triggering methods.

Figure 1 shows the X-ray light curve of Mkn421 during June 1998 (day 880 = May 31 1998). In the top panel filled circles represent one day averages WFC measurements in the 2-10 keV energy band (4-7 orbits, depending on the primary pointing). The error as given by the rms between different orbits is 20%. The first point in the plot (open circle) indicates the flux measured by the WFC during a single available orbit and the uncertainty here is correspondingly higher. The star indicates the flux seen during our observation of June 22, 1998. The dashed lines identify the flux levels recorded during two *BeppoSAX* NFI exposures on this source in 1997 (Guainazzi et al. 1998, Fossati et al. 1998). The bottom panel shows the RXTE-ASM one day average light curve in the 2-10 keV energy range (RXTE-ASM public archive). Variations of the order of a factor of two are evident on time scales of a few days. The peak near day 884 (= June 4 1998) in the ASM light curve coincides with the largest flux recorded by the *BeppoSAX* WFC. The flux of about 40-50 mCrab in June 1998 is by far the largest X-ray flux ever observed from Mkn 421. Note that in June 1998, Mkn421 was always detected in a rather high state.

The *BeppoSAX* NFI used for the observation of Mkn 421 consist of a Low Energy Concentrator Spectrometer (LECS, Parmar et al. 1997) sensitive between 0.1 and 10 keV; three identical Medium Energy Concentrator Spectrometers (MECS, Boella et al. 1997b) covering the 1.5-10 keV band; and two co-aligned high energy instruments, the High Pressure Scintillator Proportional Counter (HPGSPC, Manzo et al. 1997) and the Phoswich Detector System (PDS, Frontera et al. 1997) operating in the 4-120 keV and 15-300 keV bands respectively.

The MECS was composed at launch by three identical units. On 1997 May 6<sup>th</sup> a technical failure caused the switch off of unit MECS1. All observations after this date are performed with two units (MECS2 and MECS3). The LECS is operated during spacecraft dark time only, therefore LECS exposure times are usually smaller than the MECS ones by a factor 1.5-3. The PDS and the HPGSPC are collimated instruments with a FWHM of about 1.4 degrees. The PDS consists of four phoswich units, and is normally operated with the two collimators in rocking mode, that is with two phoswich units pointing at the source while the other two monitor the background. The two halves are swapped every

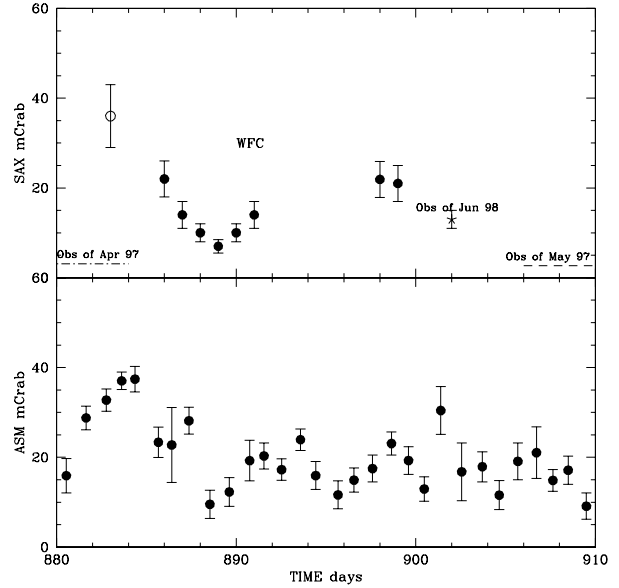


**Figure 1.** *BeppoSAX* -WFC light curve (top panel) compared with ROSSI-ASM one day average (bottom panel) during *BeppoSAX* observations of June 1998.

96 seconds. This default configuration was also used during our observation of Mkn421. The net source spectra have been obtained by subtracting the off and the on counts.

The effective exposure time was 32516 seconds in the MECS, 11082 seconds in the LECS, 13912 in the PDS and 13750 in the HPGSPC.

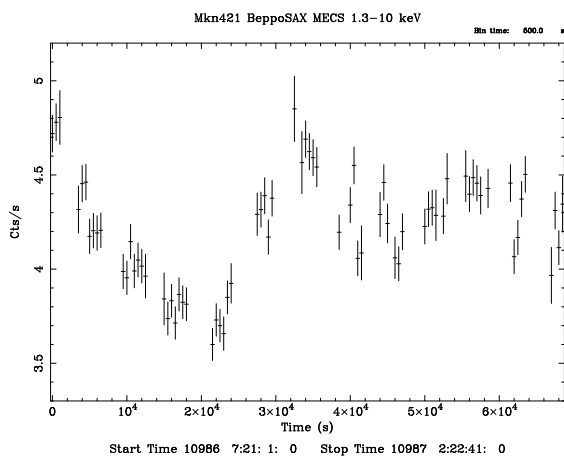
Standard data reduction was performed using the software package "SAX-DAS" (see <http://www.sdc.asi.it/software> and the Cookbook for *BeppoSAX* NFI spectral analysis, Fiore, Guainazzi & Grandi 1998). Data are linearized and cleaned from Earth occultation periods and unwanted period of high particle background (satellite passages through the South Atlantic Anomaly). The LECS, MECS and PDS background is relatively low and stable (variations of at most 30 % during the orbit) thanks to the satellite low inclination orbit (3.95 degrees). Data have been accumulated for Earth elevation angles  $> 5$  degrees and magnetic cut-off rigidity  $> 6$ ). For the PDS data we adopted a fine energy and temperature dependent Rise Time selection, which decreases the PDS background by  $\sim 40\%$ . This improves the signal to noise ratio of faint sources by about 1.5 (Frontera et al. 1997, Perola et al. 1997, Fiore, Guainazzi & Grandi 1998). Data from the four PDS units and the two MECS units have been merged after equalization and single MECS and PDS spectra have been accumulated. We extracted spectra from the LECS and MECS using 8 arcmin radius regions. LECS and MECS background spectra were extracted from blank sky fields from regions of the same size in detector coordinates.

## 3 RESULTS

**Table 1.** Mkn421 spectral fits

model (0.1-100 keV)	$\alpha_E$	$\alpha_H$	$E_0^a$	$\beta^b$	$E_f^{a,c}$	$\chi^2$ (d.o.f.)
April 1997						
PL+ABS*	2.4	–	–	–	–	2086 (136)
CurvedPL+ABS*	1.4	2.7	3.91	0.32	–	112.8 (136)
May 1997						
PL+ABS*	2.4	–	–	–	–	921.8 (136)
CurvedPL+ABS*	2.0	2.8	3.89	0.84	–	155.0 (136)
June 1998						
PL+ABS*	2.2	–	–	–	–	4027 (201)
CurvedPL+ABS*	1.8	2.4	2.7	1.08	–	291 (201)
CurvedPL+ABS*+Highecut	1.8	2.3	1.72	1.1	30	239 (201)

\* $N_H = 1.6 \times 10^{20} \text{ cm}^{-2}$  FIXED;  $a$  in keV;  $b$  = curvature radius;  $c$  Folding Energy


**Figure 2.** MECS light curve (1.3–10) keV with a binning time of 500s

### 3.1 Temporal Analysis

Figure 2 shows the MECS 1.3–10 keV light curve in bins of 500 seconds. Variations of a factor of 25% are present on time-scales of 8–10 ks (see the rise from time=24ks to time=32ks). Variations of a smaller amplitude are present down to a 500–1000 seconds timescale (see for example the events at time=24 ks, 46ks, 62ks in Figure 2). These variations are accompanied by strong spectral variability. This is shown in Figure 3, where we plot the light curves in the PDS 13–50 keV band, LECS 0.1–0.7 band, MECS “Soft” 1.3–3 keV and “hard” 5–10 keV bands, along with the MECS Hard/Soft hardness ratio (HR) (from top to bottom). The bin size used, 2850 seconds, roughly corresponds to half of the satellite orbit, and helps in illustrating how the LECS data are actually acquired for part of each orbit only. Therefore, they are not completely simultaneous to the MECS and PDS data. This can introduce an offset between the normalization in the LECS and the other instruments in spectral fits (see next section). The comparison of the light curves in different energy bands (in particular the two MECS light curves and the LECS light curve) shows that the source hardens while brightening, in agreement with the results of Giommi et al. (1990), Takahashi et al (1996) and Sambruna et al. (1996). Unfortunately, the statistics in the PDS is not

good enough to allow us to search for an extension of this trend at energies higher than 10 keV. The behaviour of the MECS HR suggests that the hard X-rays lead the soft X-rays. Figure 4 shows the 5–10 keV/1.3–3 keV hardness ratio HR plotted against the intensity (1.3–3keV + 5–10keV count rate), in bins of 5700 seconds (roughly one orbit). Numbers indicate progressive orbits. Starting from orbit number 1, the HR first decreases with decreasing count rate, and successively increases again, but at a higher rate, following a clockwise motion. Takahashi et al. (1996) found a similar behaviour in an ASCA observation, when the source was at a flux level similar or slightly higher than during our *BeppoSAX* TOO observation, indicating again that hard X-rays lead the soft X-rays. To measure the lag time we have calculated the Discrete Correlation Function (Edelson & Krolik 1988) between the MECS Soft and Hard light curves. We find a lag of  $1700 \pm 600$  seconds (90 % confidence interval).

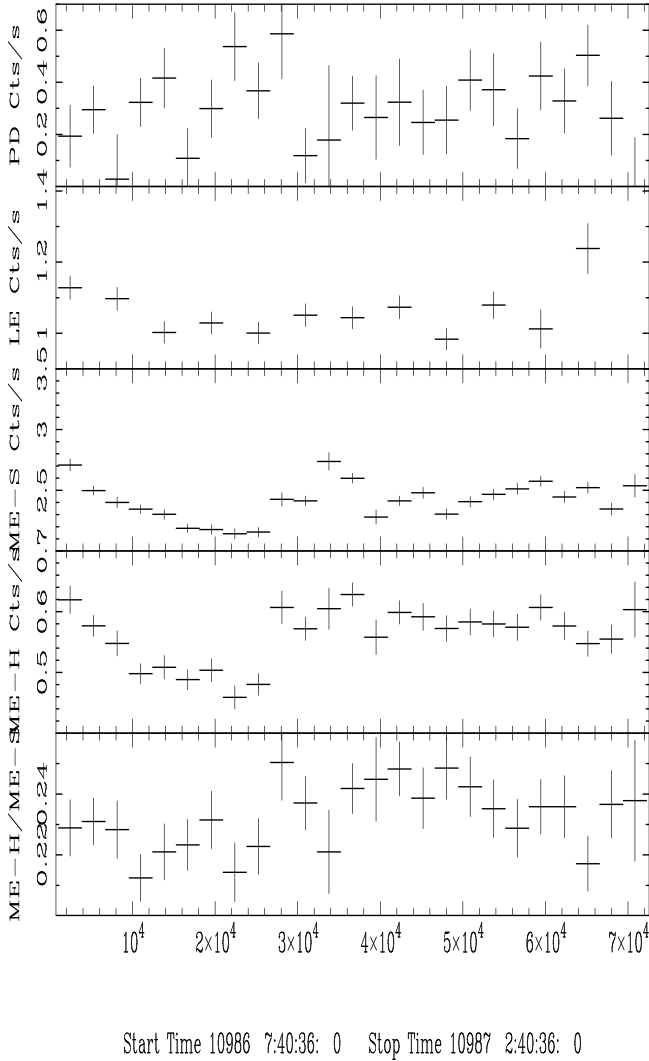
### 3.2 Spectral Analysis

Spectral fits were performed using the XSPEC 9.0 software package and public response matrices as from the 1998 November issue. PI channels are rebinned sampling the instrument resolution with the same number of channels at all energies when possible and to have at least 20 counts per bin. This guarantees the use of the  $\chi^2$  method in determining the best fit parameters, since the distribution in each channel can be considered Gaussian.

Constant factors have been introduced in the fitting models in order to take into account the intercalibration systematic uncertainties between instruments (Cusumano et al. 1999, Fiore, Guainazzi & Grandi 1998). The expected factor between LECS and MECS is about 0.9. In the fits we use the MECS as reference instruments and constrained the LECS parameter to vary in the small range 0.8–1. The expected factor for MECS and PDS is 0.8 and we constrained the PDS parameter to vary in the range 0.7–0.9.

The energy range used for the fits are: 0.1–4 keV for the LECS (channels 11–400), 1.65–10 keV for the MECS (channels 37–220) and 13–100 keV for the PDS.

Many existing narrow band X-ray spectra of blazars are sufficiently well described by a single power-law model. However recent wide band X-ray spectra of Mkn421 (Fossati

MKN 421  
Bin time: 2850. s

**Figure 3.** Light curves in the 13–50 keV (PD), 0.1–0.7 keV (LE), 1.3–3 keV (ME-H) and 5–10 keV (ME-S) and their hardness ratio (ME-H/ME-S)

et al. 1998, Guainazzi et al. 1998), PKS 2155-304 and other bright BL Lacs require more complex models like a broken power-law or a curved spectrum (e.g. Giommi et al. 1998, Wolter et al. 1998).

Figure 5 shows the *BeppoSAX* LECS, MECS, HPGSPC, PDS, 0.1–100 keV spectrum of Mkn421 measured during the June 1998 observation and fitted to a simple power-law plus low energy absorption due to a  $N_H$  column equal to the Galactic value along the line of sight. A single power-law model is clearly an unacceptable representation of the data ( $\chi^2_\nu = 23$ ). Figure 5 demonstrates that this is not due to a localized feature but to an incorrect modelling of the spectrum across the entire 0.1–100 keV energy range. In fact, the residuals plotted at the bottom of figure show that large convex spectral curvature is present.

A gradual steepening with energy is in line with the Synchrotron Self Compton (SSC) mechanism, a widely accepted scenario to explain the SED of HBL objects (Ghis-

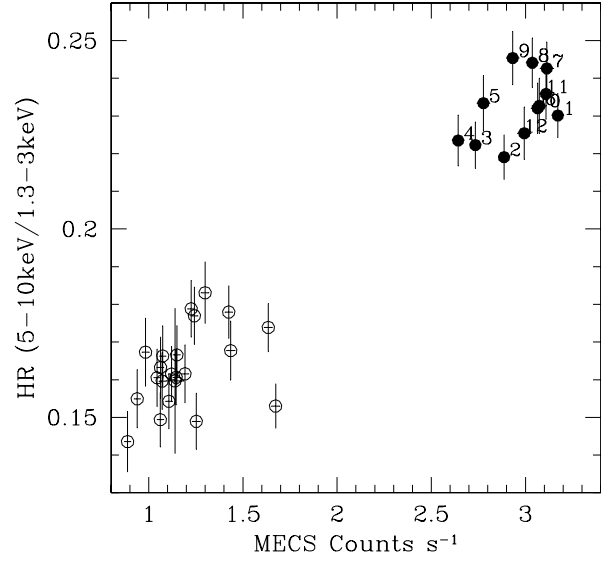


**Figure 4.** Hardness ratio (5–10 keV/1.3–3 keV) versus intensity (1.3–3 keV + 5–10 keV). In the left-bottom corner the April 97 counts have been plotted while the TOO counts are the points located in the right-top corner. The numbers put on the side of our data points indicate progressive orbit (5700s)

ellini et al. 1998). We have thus fitted our data to a *curved spectrum* (Matt, private communication) defined as follows

$$F(E) = E^{-[(1-f(E))\alpha_E + f(E)\alpha_H]}$$

where  $f(E) = [1 - \exp(-E/E_0)]^\beta$ ,  $\alpha_E$  and  $\alpha_H$  are the low and high energy asymptotic energy indices  $E_0$  is a break energy and  $\beta$  is the curvature radius. The column density has been fixed to the Galactic value along the line of sight of Mkn421 ( $N_H = 1.6 \times 10^{20} \text{ cm}^{-2}$ , Dickey & Lockman 1990). This model has been successfully applied to the previous *BeppoSAX* observation of Mkn421 (Guainazzi et al. 1998) and PKS2155-304 (Giommi et al. 1998).

This curved model gives acceptable fits to the 1997 *BeppoSAX* observations. However the June 1998 spectrum requires additional curvature; a good fit ( $\chi^2 = 189/153$ ) can be obtained adding a high energy cutoff to the model (see figure 6). The analysis of the residuals in figure 6 shows a deviation of the order of 30% below 0.5 keV, probably due to the carbon edge like feature in the LECS energy range. Moreover at lowest energies (0.1–0.2 keV) a more curved model seems to be required. The results of our spectral analysis on all the observations considered in this paper are summarized in Table 1. Our results on the April 1997 observation of Mkn421 (taken from the *BeppoSAX* public archive) are well in agreement with the original analysis presented in Guainazzi et al. (1998).

#### 4 COMPARISON WITH PREVIOUS OBSERVATIONS

*BeppoSAX* has observed Mkn421 in several campaigns be-

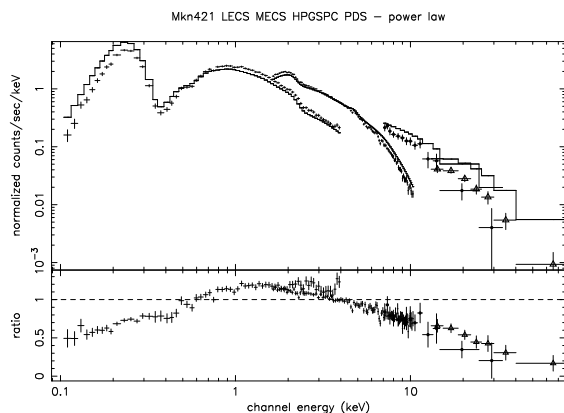


**Figure 5.** *BeppoSAX* broad band spectrum of Mkn421 during the TOO of June fitted with a simple power law. The filled circles and the triangles represent the HPGSPC and PDS data respectively.

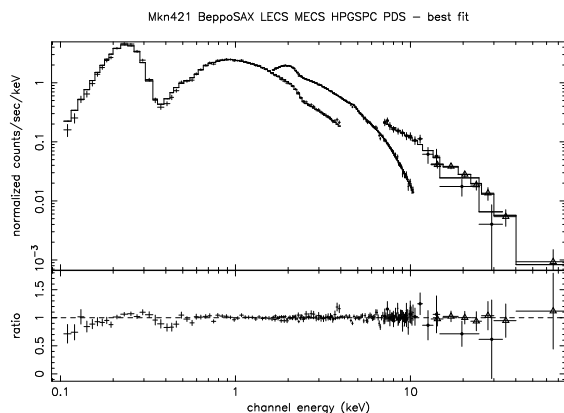


**Figure 6.** *BeppoSAX* broad band spectrum of Mkn421 during the TOO of June fitted with a curved power law plus a high energy cutoff. The filled circles and the triangles represent the HPGSPC and PDS data respectively.

tween 1997 and 1998 and in particular the April 1997 and May 1997 observations have been taken into consideration in the present work to study the spectral variations of the source.

Figure 4 compares the MECS HR measured during the June 1998 observation with that measured during three April 1997 observations, when the source was in a quiescent state (Guainazzi et al. 1998). During the April 1997 observations the HR increases with increasing intensity until it saturates (Guainazzi et al. 1998), in line with what was found in a similar quiescent state by Giommi et al. 1990 and Sambruna et al. 1994. The HR in June 1998 is much higher than during the 1997 observations, indicating that the saturation possibly concerns single variability events only. The 1998 HR does not saturate, indicating that either the observation did not catch the source at the peak of a variability cycle, or that HR saturation does not apply to variability events in high source states.

The comparison of the June 1998-TOO observation of

Mkn421 with the 1997 *BeppoSAX* observations shows strong spectral variations. In figure 7 we have plotted the ratio between the spectrum seen during our TOO observation and that during the April 97 (open squares) and May 97 (filled circles) observations. It is evident that the source hardened significantly when it brightened (up to a spectral ratio of 4-5 at 10 keV). This hardening is more pronounced above 1 keV. Below this energy the spectral ratio is less than a factor 2 showing that most of the variability occurred at high energy.

In figure 8 we report the 0.1-100 keV spectra of Mkn 421 during the three observations considered, multiplied by the frequency  $\nu$ . The maxima in this plot identify the region where most of the synchrotron power is emitted. During the high state the peak is located at  $\log \nu \sim 17.4$ , or about 1 keV, while during the other observations the peak was below 1 keV.

## 5 DISCUSSION AND CONCLUSIONS

The spectral energy distribution of high-energy peaked BL Lacs, from radio to  $\gamma$ -ray energy, in the  $\nu\nu F_\nu$  representation, is characterized by two peaks: one in the UV/soft X-ray band and the second at the GeV to TeV energies. This spectral energy distribution is generally interpreted as due to incoherent synchrotron radiation followed by Inverse Compton emission (e.g. Ghisellini, Maraschi & Dondi 1996). The radio to X-ray emission is produced by the synchrotron process as strongly suggested by the connection of the X-ray and IR, optical, UV spectra. On the contrary the inverse Compton is responsible for the  $\gamma$ -ray emission and the correlated flaring at X-ray and TeV energies (Takahashi et al. 1996). Many theoretical models have been proposed to explain the spectral and the timing variability observed in the high-energy peaked BL Lac. The comparison between different spectral states can give us information on the source electron distribution. The 1997 and the 1998 *BeppoSAX* data show both an increase in power and a shift in the synchrotron peak. This suggests that during high states the number of energetic electrons is higher and that a simple increase of the magnetic field or of the electron cutoff energy is not sufficient to explain the data. A possible explanation could be the injection of energetic electrons caused by shocks in a relativistic jet (Kirk et al. 1998). A behavior similar to that of Mkn421 has been observed in Mkn 501 (Pian et al. 1998, Ghisellini 1998) and 1ES2344+514 (Giommi et al. 1999).

On the other hand, the study of the short term variability can provide detailed information on the cooling mechanisms and the source geometry. The characteristic short time scale change of the hardness ratio as a function of the count rate and the lags between the hard and soft photons have been interpreted by Takahashi et al. (1996) in terms of Synchrotron cooling. They estimated a time lag between hard (2-7.5 keV) and soft (0.5-1 keV) energy bands of the order of one hour during an ASCA observation when the source was in a state similar to that seen during our *BeppoSAX* TOO observation. Following Takahashi et al. (1996) and assuming a  $t_{sync} \sim 1.2 \times 10^3 B^{-3/2} E_{keV}^{-1/2} \delta^{-1/2}$ , where  $E_{keV}$  is the observed energy, using their values of  $B \sim 0.2$  G and  $\delta = 5$  we have calculated that the time lag between hard (5-10 keV) and soft (1.3-3.5 keV) emission in our observation should be

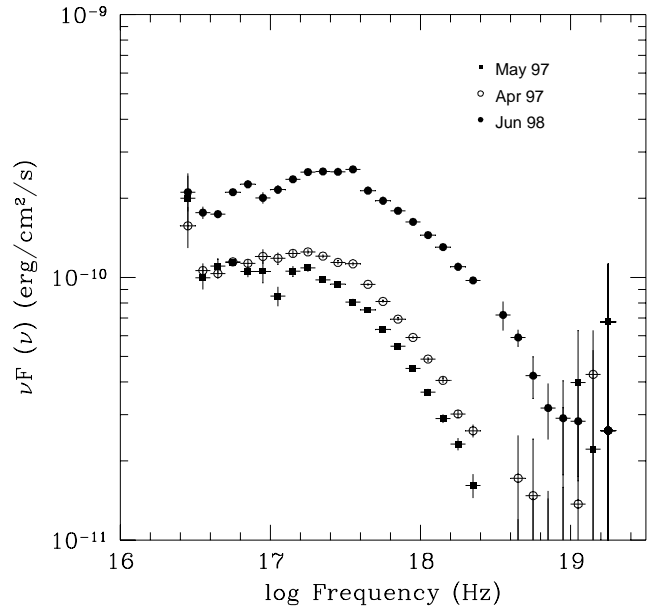


**Figure 7.** Spectral ratio of the June 1998 TOO observation to those of April 97 (open squares) and May 97 (filled circles). Both ratios increase with energy, reaching a maximum of 4-5 at 10 keV.

of about 1500 seconds ( $\sim 25$  min) which is consistent with the value found with the DCF method (see section 3.1).

In a recent work Chiaberge and Ghisellini (1999) studied the time dependent behaviour of the electron distribution injected in the emitting region and proposed a comprehensive model to describe the evolution of synchrotron and self Compton spectra. They pointed out that the cooling time can be shorter than the light crossing time ( $R/c$ ) and if this is the case the particle distribution will evolve more rapidly than  $R/c$  and the observer will see the contribution of the different spectra produced in each *slice* of the source. Taking into account the light time crossing effects, the different cooling times of electrons emitting at various frequencies can cause remarkable time delays, of the order of those observed by us and by Takahashi et al. (1996).

We thank G. Matt for providing the XSPEC gradually changing index power-law model used to fit the data in this paper.

## REFERENCES

- Boella G. et al. 1997a A&AS, 122, 299  
 Boella G. et al. 1997b A&AS, 122, 327  
 Chiaberge M. & Ghisellini G., 1999, MNRASS, in press  
 Cusumano G., et al. 1999, in preparation  
 Costa E. 1998, Nuclear Physics B (Proc. Suppl.) 69/1-3, 646  
 Dickey J.M. & Lockman F. J. 1990, ARAA, 28, 215  
 Edelson R. A. & Krolik J. H., 1988, ApJ 333, 646  
 Fossati, G., et al. 1998, Nuclear Physics B (Proc. Suppl.) 69/1-3, 423  
 Fiore F., Guainazzi M., Grandi P. 1998, *BeppoSAX Cookbook*

**Figure 8.** 0.01-100 keV spectra of Mkn421 during the three *BeppoSAX* observations, multiplied by the frequency.

- Frontera F., Costa E., Dal Fiume D., et al. 1997 A&AS, 122, 357  
 Gaidos J. A., et al. 1996, Nature, 383, 319  
 Ghisellini G., 1998, Nuclear Physics B (Proc. Suppl.) 69/1-3, 397  
 Ghisellini G., Celotti A., Fossati G. et al. 1998, MNRAS 301, 451  
 Ghisellini G., Maraschi L., and Dondi L. 1996, A&AS, 120, 503  
 Giommi P., Barr P., Garilli B., Maccagni D., Pollock T., 1990, ApJ 356, 432  
 Giommi P., Padovani P., and Perlman E., 1999 MNRAS, in press  
 Giommi P., Fiore F., Guainazzi M., et al., 1998, A&A 333, L5  
 Guainazzi M., Vacanti G., Malizia, A., et al., 1998, A&A 342, 124  
 Jager R., et al. 1997 A&AS, 122, 557  
 Kirk J. G., Rieger F. M., Mastichiadis A. 1998, A&A 333, 452  
 Manzo G., Giarrusso S., Santangelo A., et al. 1997 A&AS, 122, 341  
 Padovani, P. & Giommi, P., 1996, MNRAS 279, 526  
 Parmar A., Martin D. D. E. , Bavdaz N., et al. , 1997 A&AS 122,309  
 Perola C. 1998, Nuclear Physics B (Proc. Suppl.) 69/1-3, 477  
 Pian E., Vacanti, G., Tagliaferri G., et al., 1998 ApJ 492, L17  
 Punch M., Akerlof C. W., Cawley, M. F., et al., 1992, Nature 258, 477  
 Sambruna R. M., Barr P., Giommi P., et al. 1994, ApJS 95, 317  
 Sambruna R. M., Maraschi L., Urry C. M 1996, ApJ, 463, 444  
 Takahashi T., Tashiro M., Madejeski G., et al. 1996, ApJ 470, 89  
 Wolter A. et al., 1998 , A&A 335, 899